ORIGINAL

Hamdi Ezzin · Bin Wang · Zhenghua Qian ·
Mohammad Arefi

Multiple crossing points of Lamb wave propagating in a magneto-electro-elastic composite plate

Abstract This article is concerned with the propagation of guided type-Lamb waves in a magneto-electro-elastic composite plate. As a numerical method, the ordinary differential equation with the Thomson Haskell parameterization of Stroh formalism is employed to determine the wave characteristics in the composite plate by imposing the traction-free boundary condition on the top and bottom surfaces. Multiple crossing appears in the dispersion curves between the symmetric and the antisymmetric Lamb modes, which makes the dispersion curves more complicated and interesting to study. We are trying in this research to find, are these modes really coupled and why? For that, a set of numerical results are presented like the dispersion curves, the non-dimensional frequency, bulk waves slowness curve as well as the mechanical displacement U_1 and U_3 versus the non-dimensional thickness. These results could be interesting for the analysis and design of new acoustic devices based on magneto-electro-elastic material as well as a good candidate for nondestructive testing technology.

1 Introduction

Due to the vast applications of smart materials in aerospace, sensors and actuators transport vehicles, medical instruments, supersonic airplanes and so on. Intelligent structures made of piezoelectric and magnetostrictive materials (MEE) are nowadays widely utilized in engineering fields. In 1990s, a strong magneto-electrical coupling effect was found in two-phase structure composed of piezoelectric and piezomagnetic materials, which has wide practical application in many scientific fields [1, 2] and reported that this coupling effect cannot be found in a single-phase material. Moreover, MEE material shows important properties that the electrical polarization could be produced directly by the application of magnetic field, or indirectly the modification of the magnetic state is induced by an electric field. For these advantages, MEE have received wide applications in modern industries such as nondestructive testing, aircraft structure and vibration control. Lamb waves have been extensively studied in laboratory as in industry for many years because he has the ability to propagate through the entire thickness of the plate [3, 4]. Understanding Lamb wave behavior in composite magneto-electro-elastic material is important because it is directly related to the application in actuator/sensor technology, the nondestructive testing technology, etc.

H. Ezzin (✉) · B. Wang · Z. Qian
State Key Laboratory of Mechanics and Control of Mechanical Structures, Nanjing University of Aeronautics and Astronautics, 29 Yudao Jie, Nanjing, China
e-mail: ezzinhamdi@nuaa.edu.cn; ezzinhamdi@yahoo.fr

M. Arefi
Department of Solid Mechanics, Faculty of Mechanical Engineering, University of Kashan, Kashan 87317-51167, Iran

We studied in this paper the propagation behavior of guided type Lamb wave in composite $BaTiO_3$–$CoFe_2O_4$ with different volume fraction of $BaTiO_3$ (25%, 50% and 75%). Multiple crossing was found between symmetric and antisymmetric Lamb modes. Many researchers have studied the reason of crossing in dispersion curve. Chuanwen and Yang [5] studied Lamb wave in PMN-xPT piezoelectric plate with different anisotropies. Multiple crossings was found in dispersion curves in [001]c and [011]c polarized PMN-PT crystals plates. They attribute the multiple crossing to the multivalued slowness curves. Tomáš Grabec and al [6] apply the Ritz–Rayleigh method for the calculation of Lamb waves in extremely anisotropic media, interesting dispersion curve was found in Ni–Mn–Ga [100]-direction Plate and Ni–Mn–Ga in [110]-direction plate. Chuanwen Rui and Wenwu [7] studied Lamb and SH wave in PMN-xPT ($x = 0.29, 0.33$) single crystal plates. Multiple mode couplings appear in the dispersion curves for both the symmetric and the antisymmetric Lamb and SH wave. Solie and Auld [8] presented dispersion curves in a [001] cut cubic plate, and they have linked the splitting mode between the antisymmetric and symmetric mode to the slowness curves of bulk wave specifically on the concavity of the quasi-shear slowness curves. Chuanwen, Rui, Hui and Wenwu [9] studied the guided wave behavior in the [100] and [110] directions of 0.67Pb ($Mg_{1/3}Nb_{2/3}$)O_3–0.33PbTiO$_3$ piezoelectric plate, they attribute the multiple crossing in the dispersion curve to the moderate anisotropy of the crystal. Several other researchers have studied theoretically and experimentally the presence of crossing points in anisotropic [10, 11] and isotropic plate [12]. Understanding the dispersion behavior of Lamb waves in composite magneto-electro-elastic plates is valuable for developing new Lamb wave devices. As mentioned above, the present study is concerned with the propagation behavior of Lamb wave in magneto-electro-elastic composite material. Using the state vector approach a set of dispersion curves was plotted. Interesting phenomena found in these types of materials were the antisymmetric and symmetric guided modes coupling each other several times as wave-number increases. This paper is organized as follows: First, in Sect. 2, the ordinary differential equation is developed in case of decoupled Lamb wave, in Sect. 3 we present some numerical results: The dispersion curve plotting routines used by the MATLAB is explained. The bulk slowness curve was shown to explain the intertwining between modes. Some mechanical displacement profiles that visualize the differences between the mode families are plotted and discussed.

2 Theoretical background

Consider a transversal isotropic homogenous magneto-electro-elastic plate with thickness $h = 1$ mm, which is infinite in the (x_1, x_2) plane but finite in the vertical direction x_3. All the mechanical, piezoelectric and piezomagnetic constants are taken from the reference [13] (see Table 1). The coordinate system used in this work is shown in Fig. 1.
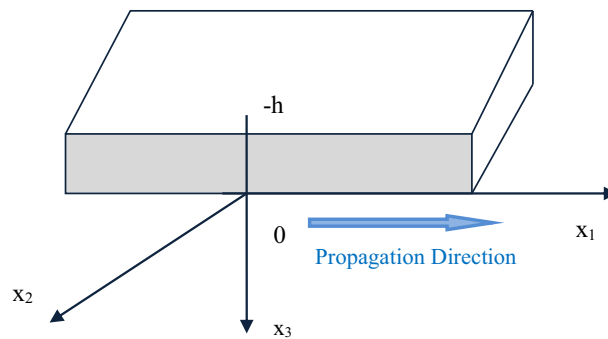

Fig. 1 Skeleton of multiferroic composite

Table 1 Materials properties of BaTiO$_3$–CoFe$_2$O$_4$ material [13]

Property	Units	v$_F$:0% (PM)	25% (MEE)	50% (MEE)	75% (MEE)	100% (PE)
C_{11}	$\times 10^9$ N/m^2	286	245	213	187	166
C_{12}	$\times 10^9$ N/m^2	173	139	113	93	77
C_{13}	$\times 10^9$ N/m^2	170	138	113	93.8	78
C_{33}	$\times 10^9$ N/m^2	269.5	235	207	183	162
C_{44}	$\times 10^9$ N/m^2	170	138	113	93.8	78
e_{31}	C/m^2	0	-1.53	-2.71	-3.64	-4.4
e_{33}	C/m^2	0	4.28	8.86	13.66	18.6
e_{15}	C/m^2	0	0.05	0.15	0.46	11.6
ε_{11}	$\times 10^{-9}$ C^2/N m^2	0.08	0.13	0.24	0.53	11.2
ε_{33}	$\times 10^{-9}$ C^2/N m^2	0.093	3.24	6.37	9.49	12.6
μ_{11}	$\times 10^{-4}$ Ns^2/C^2	5.9	3.57	2,01	0.89	0.05
μ_{33}	$\times 10^{-4}$ Ns^2/C^2	1.57	1.21	0.839	0.47	0.1
f_{31}	N/Am	580	378	222	100	0
f_{33}	N/Am	700	476	292	136	0
f_{15}	N/Am	550	331.2	185	79	0
d_{11}	$\times 10^{-12}$ Ns/VC	0	-3.09	-5.23	-6.72	0
d_{33}	$\times 10^{-12}$ Ns/VC	0	2334.15	2750	1847.49	0
ρ	$\times 10^3$ Kg/m^3	5.3	5.43	5.55	5.66	5.8

2.1 Formulation of the ordinary differential equation

The propagation of elastic waves in a magneto-electro-elastic (MEE) material will therefore be studied in the quasi-static approximation, that is to say that the magnetic energy which accompanies elastic deformation is negligible compared to electric energy. The useful equations are, then the following:

$$S_{ij} = \frac{1}{2}\left(\frac{\partial u_i}{\partial x_j} + \frac{\partial u_j}{\partial x_i}\right)$$

$$E_k = -\frac{\partial \varphi}{\partial x_k}$$

$$H_k = -\frac{\partial \psi}{\partial x_k} \tag{1}$$

where φ is the electrical potential and H the magnetic potential.

For the magneto-electro-elastic medium, the generalized constitutive relations are given as [14, 15]:

$$T_{ij} = C_{ijkl}\frac{\partial u_l}{\partial x_k} + e_{kij}\frac{\partial \varphi}{\partial x_k} + f_{kij}\frac{\partial \psi}{\partial x_k}$$

$$D_i = e_{ikl}\frac{\partial u_l}{\partial x_k} - \varepsilon_{ik}\frac{\partial \varphi}{\partial x_k} - d_{ik}\frac{\partial \psi}{\partial x_k}$$

$$B_i = f_{ikl}\frac{\partial u_l}{\partial x_k} - d_{ki}\frac{\partial \varphi}{\partial x_k} - \mu_{ik}\frac{\partial \psi}{\partial x_k} \tag{2}$$

where C_{ijkl}, ε_{ik} and μ_{ik} are the elastic, the dielectric and the magnetic permeability coefficients, respectively; e_{ikl}, f_{ikl} and d_{ik} are the piezoelectric, piezomagnetic and magneto-electric coefficients, respectively. To describe the propagation behavior of guided Lamb wave in magneto-electro-elastic (MEE) material, we use the ordinary differential equation as a method [16]. The Hooke law and the dynamic relation equation (RFD) are therefore written as a system of ordinary differential equations of the first order with non-constant coefficients of eight ranks.

$$\frac{\partial \xi}{\partial x_3} = i\omega Q\xi \quad \text{where} \quad \xi = \begin{bmatrix} i\omega U_1 \\ i\omega U_3 \\ i\omega \varphi \\ i\omega \psi \\ T_{13} \\ T_{33} \\ D_3 \\ B_3 \end{bmatrix} \tag{3}$$

where Q is the fundamental acoustic tensor, a square matrix dimensioned (8×8), which depends mainly on the physical properties and the guiding slowness component S_1, Q can be written as [17]:

$$Q = \begin{bmatrix} S_1 \Gamma_{33}^{-1} \Gamma_{31} & \Gamma_{33}^{-1} \\ S_1^2 (\Gamma_{13} \Gamma_{33}^{-1} \Gamma_{31} - \Gamma_{11}) + \rho I_4 & S_1 \Gamma_{13} \Gamma_{33}^{-1} \end{bmatrix} \tag{4}$$

I_4 Is the (4×4) identity matrix, S_1 denoting the first component of the slowness vector. The parameter ρ is the density of the material and Γ_{ik} are the (4×4) matrices formed from the elastic constants C_{ijkl}, piezoelectric constant e_{kij}, piezomagnetic constants f_{kij}, dielectric permittivity ε_{ik}, magnetic permeability constants μ_{ik} and magneto-electric coupling coefficient d_{ik}.

$$\Gamma_{ik} = \begin{bmatrix} C_{1i1k} & C_{1i3k} & e_{k1i} & f_{k1i} \\ C_{3i1k} & C_{3i3k} & e_{k3i} & f_{k3i} \\ f_{i1k} & f_{i3k} & -\varepsilon_{ik} & -\mu_{ik} \\ f_{i1k} & f_{i3k} & -d_{ik} & -\mu_{ik} \end{bmatrix} \tag{5}$$

The solution of this differential equation is a transfer matrix M which relates the state vector at $x_3 = 0$ and $x_3 = -h$.

$$\xi(x_3 = 0) = M \, \xi(x_3 = -h), \quad M = e^{iQh} \tag{6}$$

To solve the system of differential equations for a particular direction is in fact to find the eigenvalues and the eigenvectors of the matrix Q. This routine is done numerically by the "**eig**" function of the MATLAB software. There are eight of these which correspond to eight partial waves. Four waves propagate to the positive x_3. Their eigenvalues represent the third component of the wave vector k_3^{+j} and their corresponding eigenvector matrix denoted $V^+ = \begin{bmatrix} P_j^+ \\ D_j^+ \end{bmatrix}$, or P_j^+ correspond to the polarization of these waves and D_j^+ represent the stresses. The other four waves propagating toward the negative x_3, their eigenvalues k_3^{-j} and the matrix of the corresponding eigenvectors is denoted by $V^- = \begin{bmatrix} P_j^- \\ D_j^- \end{bmatrix}$ $(j = 1, 2, 3$ and $4)$. Indeed, the diagonalized form of the matrix Q is represented by:

$$Q = V \beta_{x_3}^+ V^{-1} = \begin{bmatrix} P_j^- & P_j^+ \\ D_j^- & D_j^+ \end{bmatrix} \begin{bmatrix} \beta_z^- & 0 \\ 0 & \beta_z^+ \end{bmatrix} \begin{bmatrix} P_j^- & P_j^+ \\ D_j^- & D_j^+ \end{bmatrix}^{-1} \tag{7}$$

where $\beta_{x_3}^+ = I \, \mathrm{diag}\left(k_{x_3}^{1+}, k_{x_3}^{2+}, k_{x_3}^{3+}, k_{x_3}^{4+} \right)$.

From (3) and (6)

$$\Rightarrow \quad M = V e^{iQ\beta_{x_3}} V^{-1}$$

$$\Rightarrow \quad M = \begin{bmatrix} P_j^- & P_j^+ H_j^+ \\ D_j^- & D_j^+ H_j^+ \end{bmatrix} \begin{bmatrix} P_j^- H_j^- & P_j^+ \\ D_j^- H_j^- & D_j^+ \end{bmatrix}^{-1} \tag{8}$$

From Eq. (6) we obtain:

$$\begin{bmatrix} i\omega U(x_3 = -h) \\ T(x_3 = -h) \end{bmatrix} = M \begin{bmatrix} i\omega U(x_3 = 0) \\ T(x_3 = 0) \end{bmatrix} \tag{9}$$

2.2 Boundary conditions

The boundary conditions for the propagation of Lamb waves in homogeneous magneto-electro-elastic plate requires that the normal and tangential component of the stress, electric and magnetic displacement, magnetic and electric potential should vanish at the upper and lower surfaces.

Electrically open and magnetically close conditions (denoted by "os"): [18, 19]

$$
\begin{aligned}
&\text{At } x_3 = 0 \\
&\tau_{13} = \tau_{33} = D_3 = B_3 = 0 \\
&\text{At } x_3 = -h \\
&\tau_{13} = \tau_{33} = D_3 = B_3 = 0
\end{aligned}
\tag{10}
$$

Electrically shorted and magnetically open conditions (denoted by "so"): [18, 19]

$$
\begin{aligned}
&\text{At } x_3 = 0 \\
&\tau_{13} = \tau_{33} = \varphi = \psi = 0 \\
&\text{At } x_3 = -h \\
&\tau_{13} = \tau_{33} = \varphi = \psi = 0
\end{aligned}
\tag{11}
$$

2.3 Solution

By developing Eq. (9) we obtain: [20]

$$
\begin{pmatrix} i\omega U_1 \\ i\omega U_3 \\ i\omega\varphi \\ i\omega\psi \\ T_{13} \\ T_{33} \\ D_3 \\ B_3 \end{pmatrix}_0 = \begin{pmatrix} Q_{11}^{os} & Q_{12}^{os} \\ Q_{21}^{os} & Q_{22}^{os} \end{pmatrix} \begin{pmatrix} i\omega U_1 \\ i\omega U_3 \\ i\omega\varphi \\ i\omega\psi \\ T_{13} \\ T_{33} \\ D_3 \\ B_3 \end{pmatrix}_{-h}
\tag{12}
$$

$$
\begin{pmatrix} i\omega U_1 \\ i\omega U_3 \\ D_3 \\ B_3 \\ T_{13} \\ T_{33} \\ i\omega\varphi \\ i\omega\psi \end{pmatrix}_0 = \begin{pmatrix} Q_{11}^{so} & Q_{12}^{so} \\ Q_{21}^{so} & Q_{22}^{so} \end{pmatrix} \begin{pmatrix} i\omega U_1 \\ i\omega U_3 \\ D \\ B_3 \\ T_{13} \\ T_{33} \\ i\omega\varphi \\ i\omega\psi \end{pmatrix}_{-h}
\tag{13}
$$

Developing Eqs. (12) and (13) as well as introducing the boundary conditions we obtain:

$$
0 = Q_{21}^{os} \begin{pmatrix} i\omega u_1 \\ i\omega u_3 \\ i\omega\varphi \\ i\omega\varphi \end{pmatrix}
\tag{14}
$$

$$
0 = Q_{21}^{so} \begin{pmatrix} i\omega u_1 \\ i\omega u_3 \\ D_3 \\ B_3 \end{pmatrix}
\tag{15}
$$

We obtain a homogeneous system of Eqs. (14, 15). In order to obtain the nontrivial solutions of the above equations (Eqs. 14–15), the determinant of $Q_{21}^{os,so}$ must vanish. So, the dispersive behaviors for the magneto-electrical open and shorted case can be investigated.
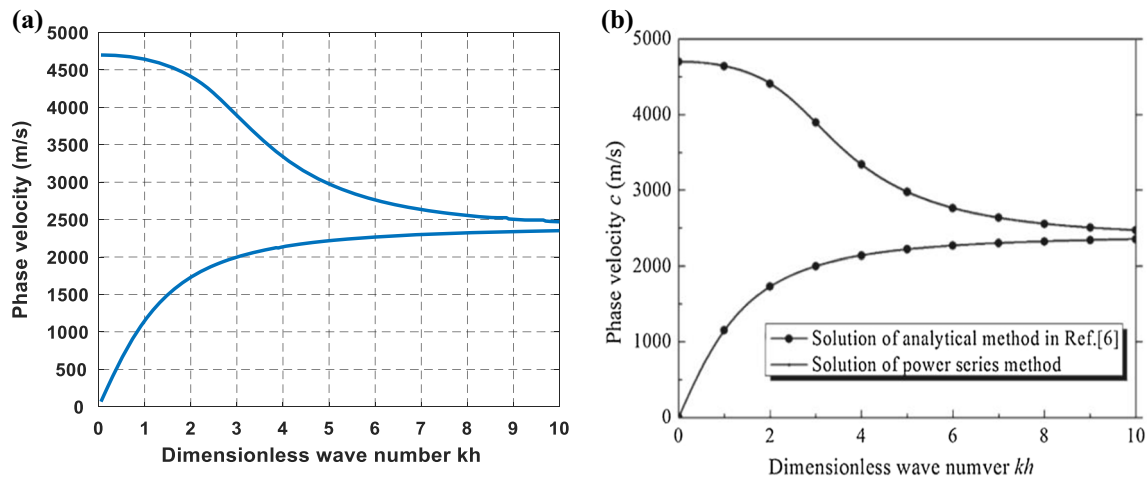
Fig. 2 Dispersion curves of S_0 and A_0 modes of homogeneous composite material, for magneto-electrically open case: **a** author result, **b** result from [21]

3 Results and discussion

3.1 Validation of the formulation

The authors of this research confirm that the unusual behavior of the dispersion curve found for the first time in these types of magneto-electro-elastic composite materials requires a validation of our calculation programs.

So, the dispersion curves of S_0 and A_0 modes of homogeneous composite material from reference [21] were plotted. Indeed, by comparing the result obtained by our method with this obtained by the power series method used by Cao et al. [21], we find that the two dispersion diagrams perfectly agree as shown in Fig. 2.

3.2 Results and discussion

In this section, the numerical evaluation is carried out using MATLAB software to assess the dispersion curves of the Lamb wave in homogenous $BaTiO_3$ piezoelectric material, $CoFe_2O_4$ piezomagnetic material and composite magneto-electro-elastic $BaTiO_3$–$CoFe_2O_4$ with the different volume fraction of $BaTiO_3$ ($\delta = 25\%, 50\%$ and 75%). In this section, we represent the phase velocity and the non-dimensional frequency versus the non-dimensional wave-number. The non-dimensional frequency is defined as follows: $\Omega = \omega h \sqrt{C_{max}/\rho}$, with C_{max} is the highest value of the elastic matrix.

The velocities of the most Lamb wave's modes decrease rapidly with frequency, then after passing a minimum tend to the shear wave velocity. As shown in Fig. 3a–d the dispersion nature in the piezoelectric $BaTiO_3$ homogenous plate and $CoFe_2O_4$ piezomagnetic homogenous plate are regular. Contrariwise multiple mode coupling appears in the dispersion curves for both the dilatational and flexural Lamb mode as they approach the surface wave limit for the $BaTiO_3$–$CoFe_2O_4$ composite with volume fraction $\delta = 25\%, 50\%, 75\%$. We are trying in this research to answer two important questions:

- Is there a relationship between the nature of the material (piezoelectric/piezomagnetic/magneto-electric) and the intersection between the symmetric and antisymmetric modes?
- "Are these modes really coupled or no"?

To answer the first question we presented in Fig. 4 the dispersion curves for $CoFe_2O_4$–$BaTiO_3$ composite plates with volume fraction ($\delta = 25\%, 50\%, 75\%$) with and without the magneto-electric coefficient. It is found that the vanish of the piezoelectric and piezomagnetic coefficients decreases the phase velocity of all Lamb modes, whereas the crossing between the modes remains unchanged except for the higher modes for the composite 75% $BaTiO_3$–25% $CoFe_2O_4$ or the number of crossing points between the modes decreases. So the splitting between A_n and S_n mode cannot be attributed to the piezoelectric and piezomagnetic nature of composite material. Solie and Auld [8] attribute the splitting between the antisymmetric and symmetric
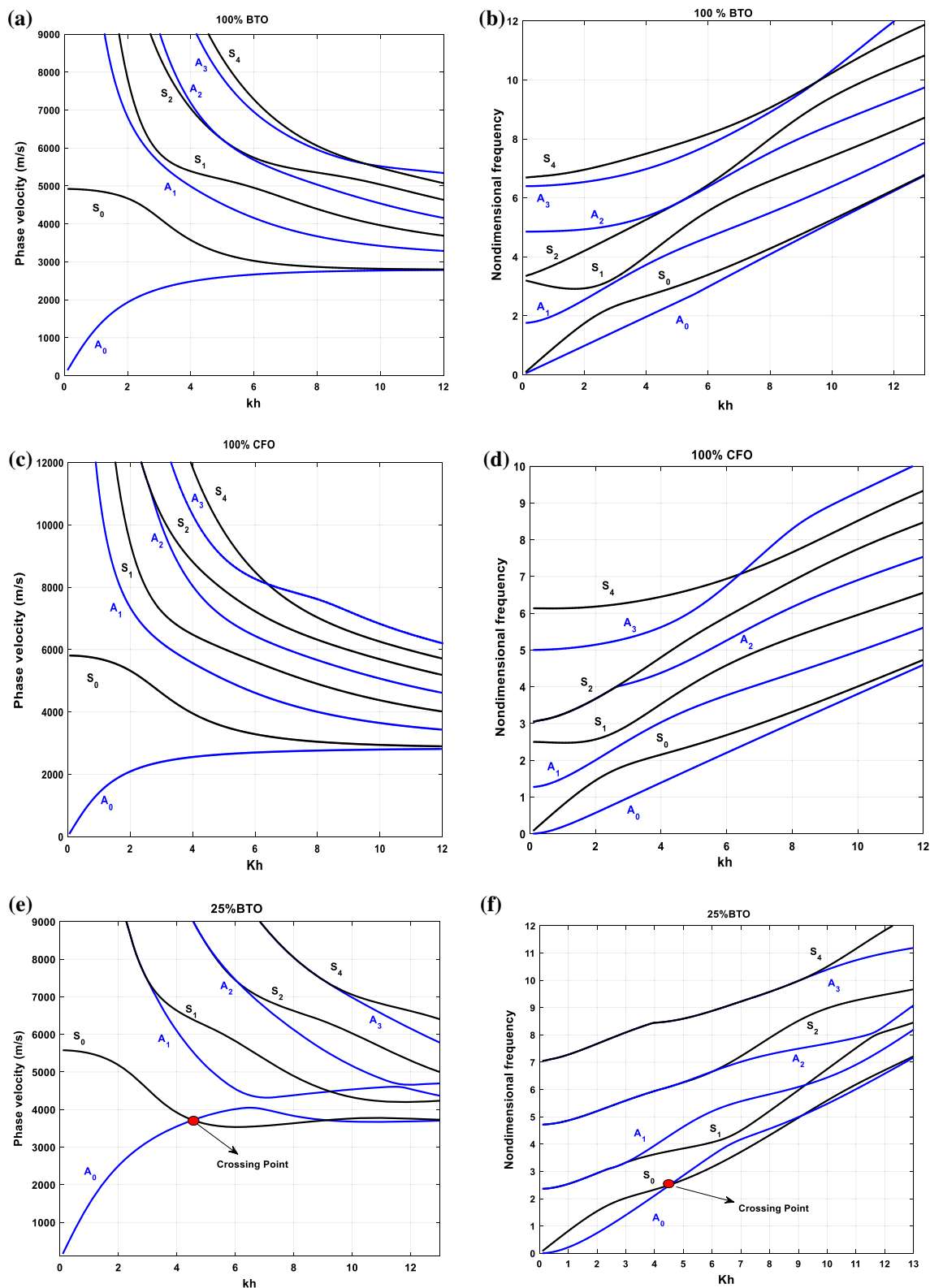
Fig. 3 a–j Dispersion curves for CoFe$_2$O$_4$–BaTiO$_3$ plates with different volume fraction of BaTiO$_3$ ($\delta = 0\%$, 25%, 50%, 75% and 100%)
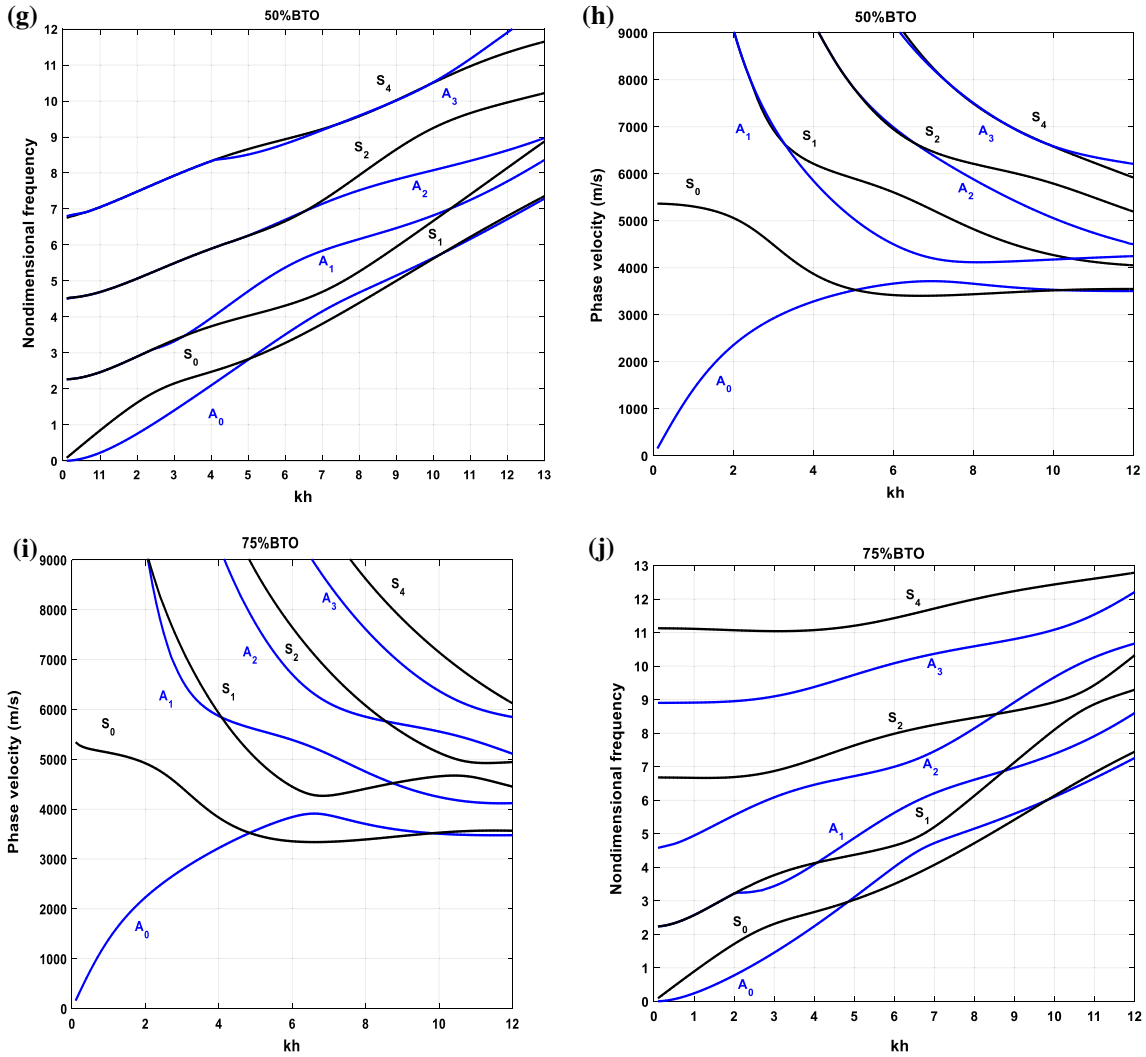
Fig. 3 continued

mode to the behavior of the slowness curve, precisely to the concavity of the quasi-shear slowness curves for "non-piezoelectric" material.

Under MATLAB R 2016a software a computational program was written to plot the slowness curves in YZ [0 1 0; − 1 0 0; 0 0 1] sagittal plane. Figures 5 show the slowness curves for all materials with different volume fraction δ. The slowness surface noted "m" (inverse of the phase velocity) characterizes the free propagation of the elastic waves in a solid and indicates the direction of propagation of the energy. It is the place of the ends of the vector $\vec{m} = \vec{n}/V$ where n is the direction of propagation. The slowness surface generally consists of three tablecloths relating to a quasi-longitudinal mode and two quasi-shears ones. The slowness curves of $BaTiO_3$ material are all circles, indicating that the slowness (and hence phase velocity) is independent of propagation direction of waves polarized in this plane, for the $CoFe_2O_4$ material we have little anisotropy in the quasi-shear partial wave. By cons the magneto-electro-elastic composite materials are strongly anisotropic (particularly in the quasi-shear partial wave). The concavity of quasi-shear velocity curves indicate high anisotropy of the material and can be an explanation of the oscillation of symmetric and antisymmetric modes as they approach their asymptotic limit. To the author's knowledge few researchers answer the question "are these modes really coupled or not?". To explain the phenomenon in Fig. 6, a succession of mechanical displacement profile u_1 and u_3 through the non-dimensional thickness has been presented.
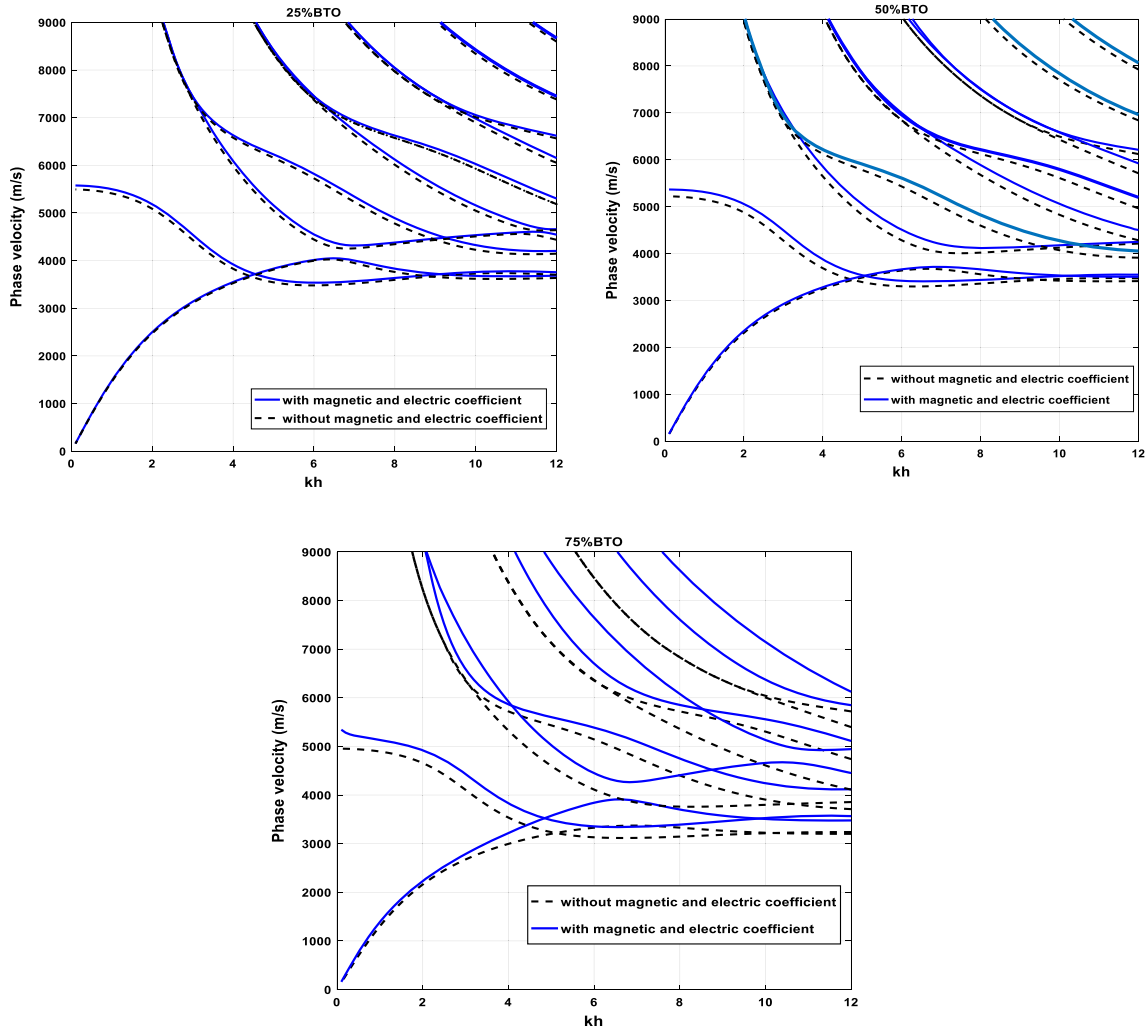
Fig. 4 Dispersion curves for CoFe$_2$O$_4$–BaTiO$_3$ plates with volume fraction of BaTiO$_3$ ($\delta = 25\%$, 50%, 75%) with magnetic and electric coefficient and without magnetic and electric coefficient

The classification of the symmetric and antisymmetric Lamb modes is deduced from the symmetries of the displacements u$_1$ and u$_3$ with respect to the median plane of the plate. The displacements of the antisymmetric modes are of the type:

$$\begin{Bmatrix} U_1(x_3) = -U_1(-x_3) \\ U_3(x_3) = U_3(-x_3) \end{Bmatrix} \tag{16}$$

The displacements of the symmetric modes are of the type:

$$\begin{Bmatrix} U_1(x_3) = U_1(-x_3) \\ U_3(x_3) = -U_3(-x_3) \end{Bmatrix} \tag{17}$$

Figure 7 shows that the displacement profiles u$_1$ and u$_3$ of A$_0$ mode before the crossing point at $kh = 4$ and after the crossing point at $kh = 6$ retains its antisymmetrical nature, which proves the intersection phenomenon between these two modes.

As for the A_0 mode, Fig. 8 shows that the displacement profiles u_1 and u_3 of the S_0 mode before the crossing point at $kh = 4$ and after the crossing point at $kh = 6$ retain its symmetrical nature, which proves the intersection phenomenon of the A_0 and S_0 modes.
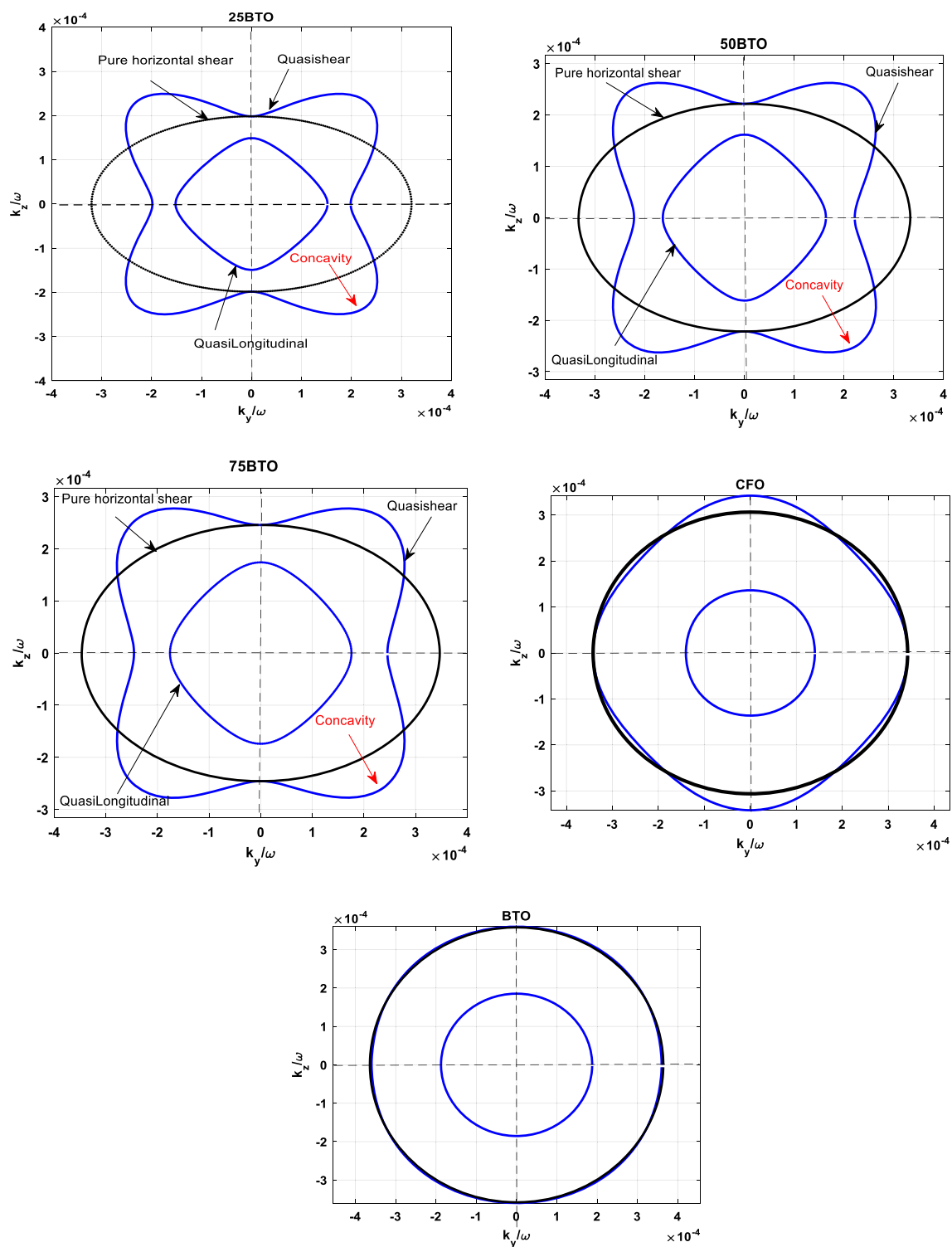
Fig. 5 Bulk wave slowness curves for propagation in BaTiO$_3$, CoFe$_2$O$_4$, 25%BTO, 50%BTO and 75%BTO without electrical and magnetically partial waves
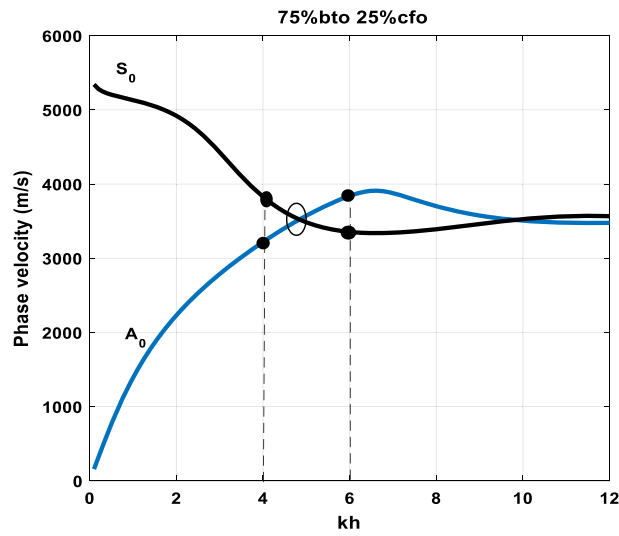
Fig. 6 Dispersion curve of the fundamental Lamb wave in 75%BaTiO$_3$–25% CoFe$_2$O$_4$ magneto-electro-elastic composite material
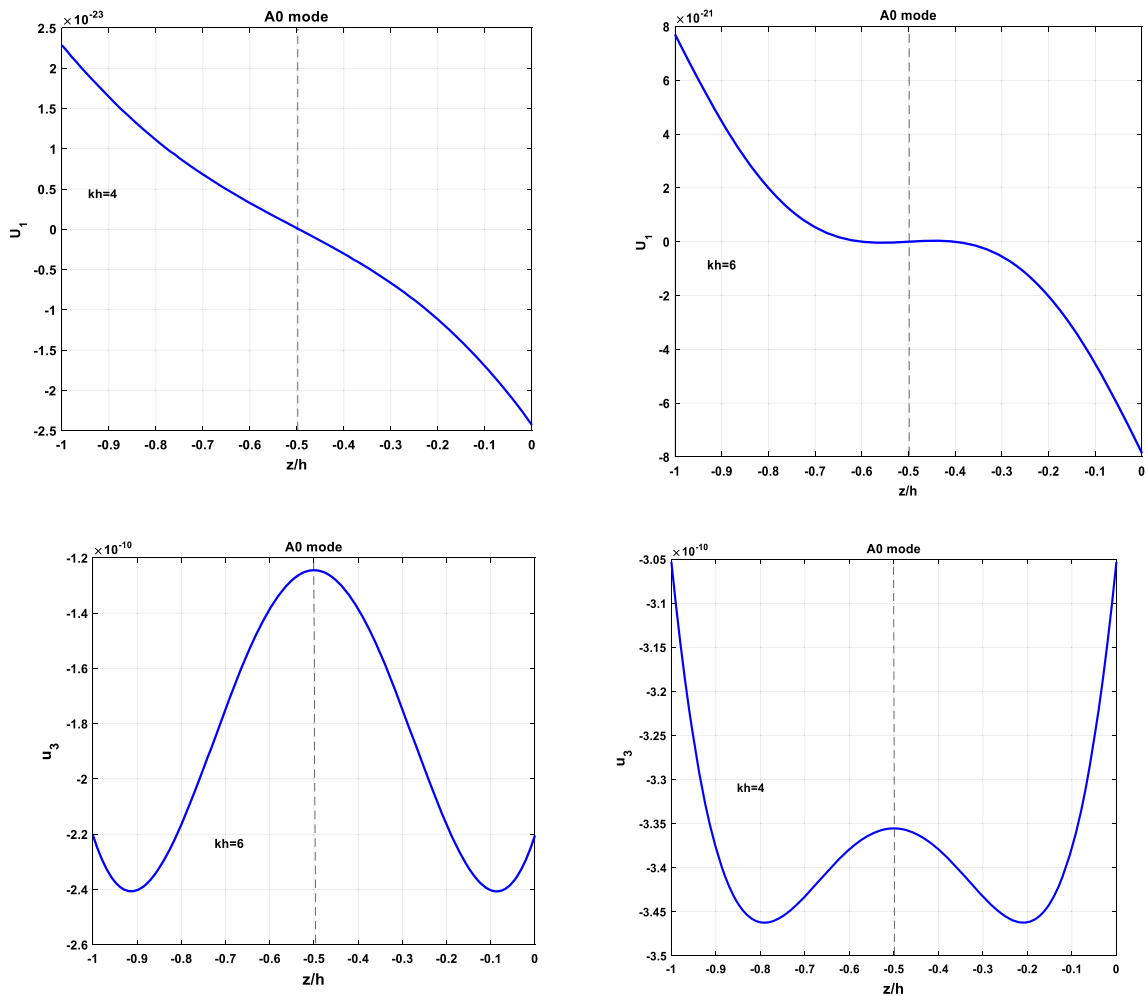

Fig. 7 Mechanical displacements for the fundamental antisymmetric Lamb mode A_0 before the crossing point at $kh = 4$ and after the crossing point at $kh = 6$
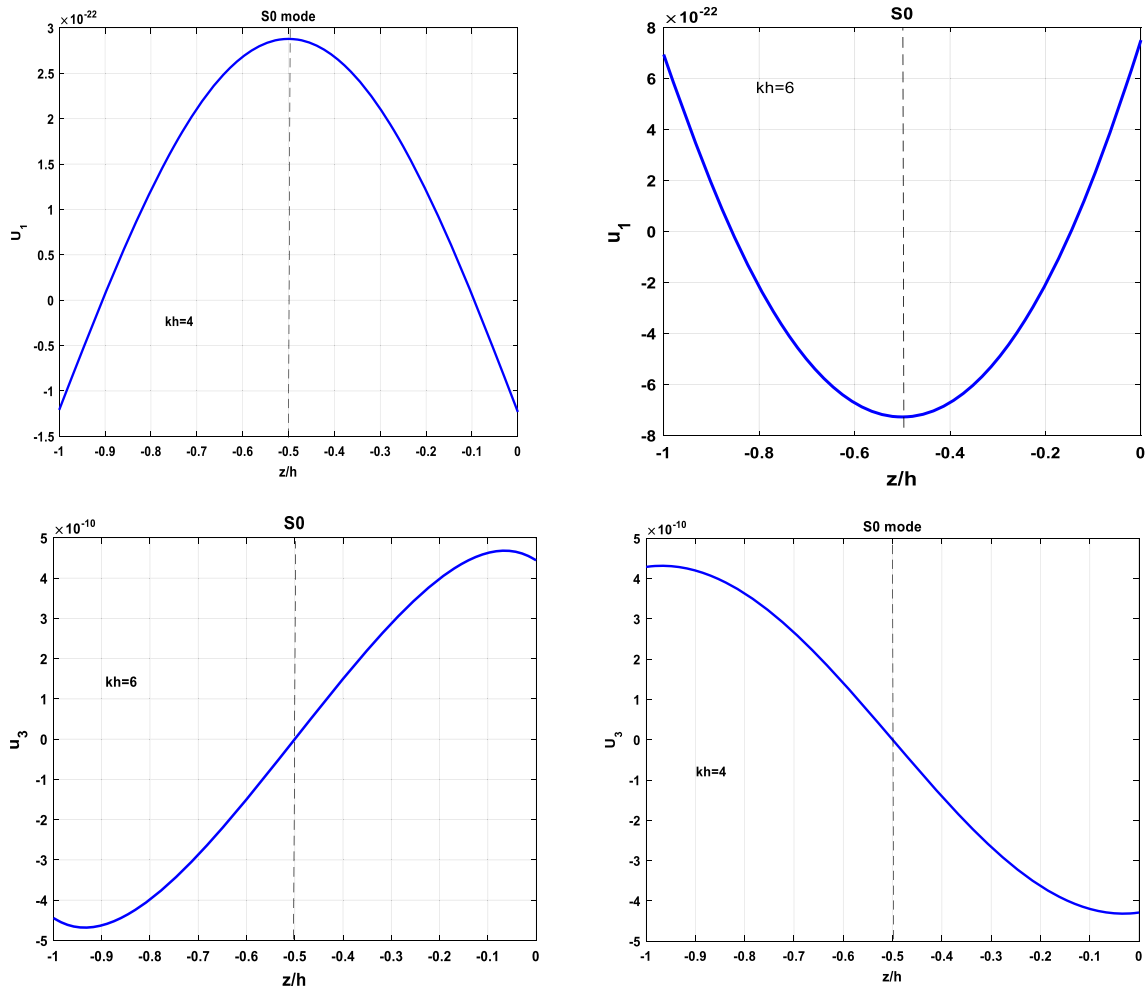
Fig. 8 Mechanical displacements for the fundamental symmetric Lamb mode S_0 before at $kh = 4$ and after the crossing point at $kh = 6$

4 Conclusion

In this research, we analyze in detail the problem of propagation of Lamb wave in magneto-electro-elastic composite plate. The dispersion curves (phase velocity and non-dimensional frequency versus non-dimensional wave-number) were plotted. Multiple intertwining modes were found in the dispersion curve which makes it both complex and important. The crossing between acoustic modes is awarded to the moderate anisotropy of the magneto-electro-elastic (MEE) composite explained by the bulk slowness curve. Finally, a succession of mechanical displacement profiles was shown to prove the crossing between the A_n and S_n mode.

Compliance with ethical standards

Conflict of interest The authors declare that they have no known competing financial interests or personal relationships that could have appeared to influence the work reported in this paper.

References

1. Harshe, G., Dougherty, J., Newnham, R.: Theoretical modelling of multilayer magnetoelectric composites. Int. J. Appl. Electromagn. Mater. **4**(2), 145 (1993)
2. García-Arribas, A., Gutiérrez, J., Kurlyandskaya, G.V., Barandiarán, J.M., Svalov, A., Fernández, E., Lasheras, A., de Cos, D., Bravo-Imaz, I.: Sensor applications of soft magnetic materials based on magneto-impedance, magneto-elastic resonance and magneto-electricity. Sensors **14**, 7602–7624 (2014)
3. Ezzin, H., Ben Amor, M., Ben Ghozlen, M.H.: Lamb waves propagation in layered piezoelectric/piezomagnetic plates. Ultrasonics **76**, 63–69 (2017)
4. Nandyala, A.R., Darpe, A.K., Singh, S.P.: Effective stiffness matrix method for predicting the dispersion curves in general anisotropic composites. Arch. Appl. Mech. **89**, 1923–1938 (2019)
5. Chen, C., Xiang, Y.: Crossing characteristics of lamb wave modes in [001]c and [011]c polarized $Pb(Mg_{1/3}Nb_{2/3})O_3$-$PbTiO_3$ crystal plates. Phys. B **407**, 1099–1103 (2012)
6. Grabec, T., Sedlák, P., Seiner, H.: Application of the Ritz–Rayleigh method for Lamb waves in extremely anisotropic media. Wave Motion **96**, 102567 (2020)
7. Chen, C., Zhang, R., Cao, W.: Theoretical study on guided wave propagation in $(1-x)Pb(Mg1/3Nb_2/3)O_3–xPbTiO_3$ (x =0.29 and 0.33) single crystal plates. J. Phys. D Appl. Phys. **42**(6), 095411 (2009)
8. Solie, L.P., Auld, B.A.: Elastic waves in free anisotropic plates. J. Acoust. Soc. Am. **54**, 50 (1973)
9. Chen, C., Zhang, R., Chen, H., Cao, W.: Guided wave propagation in $0.67PbMg1/3Nb_2/3O_3–0.33PbTiO_3$ single crystal plate poled along [001]c. Appl. Phys. Lett **91**, 102907 (2007)
10. Zhu, Q., Mayer, W.G.: On the crossing points of Lamb wave velocity dispersion curves. J. Acoust. Soc. Am. **93**, 1893 (1993)
11. Every, A.G.: Intersections of the Lamb mode dispersion curves of free isotropic plates. J. Acoust. Soc. Am. **139**, 1793 (2016)
12. István, A., Veres, T.B., Grünsteidl, C., Burgholzer, P.: On the crossing points of the Lamb modes and the maxima and minima of displacements observed at the surface. Ultrasonics **54**, 759–762 (2014)
13. Narendar, S.: Wave dispersion in functionally graded magneto-electro-elastic nonlocal rod. Aerosp. Sci. Technol. **51**, 42–51 (2016)
14. Benveniste, Y.: Magnetoelectric effect in fibrous composites with piezoelectric and piezomagnetic phases. Phys. Rev. B **51**, 16424 (1995)
15. Milan, A.G., Ayatollahi, M.: Transient analysis of multiple interface cracks between two dissimilar functionally graded magneto-electro-elastic layers. Arch. Appl. Mech. **90**, 1829–1844 (2020)
16. Shuvalov, A.L., Le Clézio, E., Feuillard, G.: The state-vector formalim and the Peano-series solution for modelling guided waves in functionally graded anisotropic piezoelectric plates. Int. J. Eng. Sci. **46**, 929–947 (2008)
17. Cécile Baron: Le Developpement en serie de Peano du matricant pour l'etude de la propagation des ondes elastiques en milieux a proprieties continument variables. Ph. D. Defended on: October 7 (2005)
18. Alshits, V.I., Darinskii, A.N., Lothe, J.: On the existence of surface waves in half-infinite anisotropic elastic media with piezoelectric and piezomagnetic properties. Wave Motion **16**, 265–283 (1992)
19. Ezzin, H., Wang, B., Qian, Z.: Propagation behavior of ultrasonic Love waves in functionally graded piezoelectric-piezomagnetic materials with exponential variation. Mech. Mater. **148**, 103492 (2020)
20. Ezzin, H., Ben Amor, M., Ben Ghozlen, M.H.: Propagation behavior of SH waves in layered piezoelectric/piezomagnetic plates. Acta Mech. **2283**, 1071–1081 (2017)
21. Cao, X., Shi, J., Jin, F.: Lamb wave propagation in the functionally graded piezoelectric–piezomagnetic material plate. Acta Mech. **223**, 1081–1091 (2012)